

# Transient Relativistic Ejections and Stationary Core in XTE J1752–223

J. Yang<sup>1\*</sup>, Z. Paragi<sup>1,2</sup>, S. Corbel<sup>3</sup>, L.I. Gurvits<sup>1,4</sup>, R.M. Campbell<sup>1</sup>, C. Brocksopp<sup>5</sup>

<sup>1</sup>*Joint Institute for VLBI in Europe, Postbus 2, 7990 AA Dwingeloo, The Netherlands*

<sup>2</sup>*MTA Research Group for Physical Geodesy and Geodynamics, POB 91, H-1521 Budapest, Hungary*

<sup>3</sup>*Université Paris 7 Denis Diderot and Service d'Astrophysique, UMR AIM, CEA Saclay, F-91191 Gif-sur-Yvette, France*

<sup>4</sup>*Department of Astrodynamics & Space Missions, Delft University of Technology, Kluyverweg 1, 2629 HS Delft, The Netherlands*

<sup>5</sup>*Mullard Space Science Laboratory, University College London, Holmbury St Mary, Dorking, Surrey RH5 6NT, UK*

Accepted 2011 August xx. Received 2011 July 20; in original form 2011 August xx

## ABSTRACT

The Galactic X-ray transient XTE J1752–223 was shown to have properties of black hole binary candidates. As reported in our previous paper, we identified transient and decelerating ejecta in multi-epoch Very Long Baseline Interferometry (VLBI) observations with the European VLBI Network (EVN) and the NRAO Very Long Baseline Array (VLBA). Here we present new EVN and VLBA data in which a new transient ejection event and later a stationary component are identified. The latter is interpreted as a reappearance of the radio core/compact jet during the transition from soft to hard X-ray state. This component appears to be highly variable in brightness although effects of tropospheric instabilities might play a role too. We also re-analyze the earlier VLBI data and find that the transient ejecta closer to the core position has significantly higher proper motion, further strengthening the case for strongly decelerating ejecta on the scale of several hundred milli-arcsecond, never observed in X-ray binaries before. Although the distance of the source is not well constrained, it is clear that these ejectas are at least mildly relativistic at the early stages. Moreover, we show the large scale environment of the transient from the Westerbork synthesis array data recorded in parallel during the EVN run.

**Key words:** stars: individual: XTE J1752–223 – stars: variable: others – ISM: jets and outflows – radio continuum: stars – X-rays: binaries.

## 1 INTRODUCTION

The X-ray transient XTE J1752–223 was discovered by the *Rossi X-ray Timing Explorer* (*RXTE*) on 2009 October 23. The 2010 outburst of XTE J1752–223 was monitored by the *RXTE* (Shaposhnikov et al. 2010), the *Monitor of All-sky X-ray Image* (*MAXI*, Nakahira et al. 2010), and *Swift* (Curran et al. 2010) in the X-ray domain. The outburst exhibited an evolving behavior in agreement with what would be expected from a stellar mass black hole binary.

In the preceding low-hard X-ray state, the radio counterpart was identified by the ATCA (Australia Telescope Compact Array) with a flux density of  $\sim 2$  mJy and a flat spectrum consistent with that of a compact jet (Brocksopp et al. 2009). XTE J1752–223 started to transit toward a high-soft X-ray state around 2010 January 20

(e.g. Shaposhnikov et al. 2010). A 10-fold increase of radio flux density and a flat spectrum were observed by the ATCA on 2010 January 21 (Brocksopp et al. 2010). The increased flux density suggested that a major ejection was imminent (Brocksopp et al. 2010) and, indeed, a transient jet was detected by the rapid-response EVN (European VLBI Network) observations on 2010 February 11. The transitions from a low-hard X-ray state toward a high-soft X-ray state are in fact, commonly associated with discrete ejection events (Corbel et al. 2004; Fender et al. 2004, 2009). Together with follow-up VLBA (Very Long Baseline Array) observations in 2010 February, the transient jet was found to show significant deceleration, possibly due to the jet interaction with the surrounding medium (Yang et al. 2010, hereafter Paper I).

In this paper we present results from the additional three epochs that show a new transient ejection event and later a stationary feature which we identify as the core. The

\* E-mail: yang@jive.nl

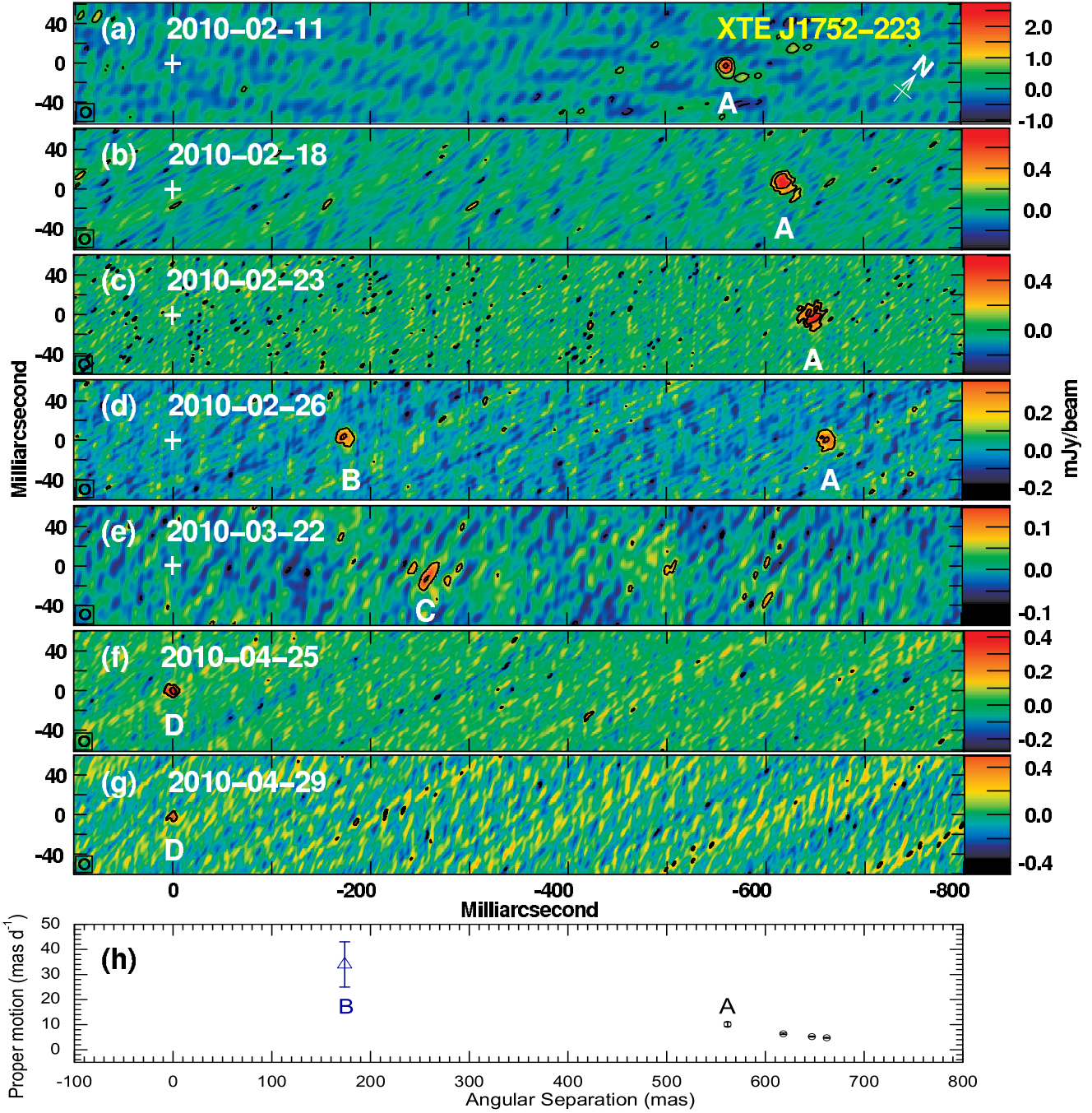


**Figure 1.** VLBI images of the transient jets components A, B, C, and the re-activated compact jet D in XTE J1752–233. The bottom panel shows the proper motion versus angular separation for components A and B. All the images are centred at the compact jet (0,0) and rotated clockwise by  $39^\circ$ . The linear scale is  $3.5 \text{ au mas}^{-1}$  at the adopted distance of 3.5 kpc. The contours start from  $3\sigma$  off-source noise level and increase by a factor of -1, 1, 2, 4. The size of the restoring beam is 10 mas.

observations and data reduction are briefly described in Section 2. The Very Long Baseline Interferometry (VLBI) as well as the Westerbork Synthesis Radio Telescope (WSRT) imaging results are presented in Section 3. The proper motion of a transient ejecta detected in one of our earlier observations is analyzed in Section 4. We discuss our results on the compact jet region, the proper motion of the transient ejecta and their possible interaction with the large-scale medium in Section 5.

## 2 OBSERVATIONS AND DATA REDUCTION

All the VLBI experiments observed at 5 GHz during the 2010 outburst of XTE J1752–223 are listed in Table 1. The observations before March 2010 were already presented in Paper I. Additional EVN observations were carried out on 2010 March 22, including Effelsberg, the phased array WSRT, Onsala, Medicina, Noto, Toruń, and the Lovell telescope. There were two epochs of VLBA observations on 2010 April 25 and 29 using the whole telescope array.

**Table 1.** The characteristics of VLBI images in Figure 1.

Map	Date (yy-mm-dd)	Array	$N_{\text{ant}}$	$t_{\text{obs}}$ (h)	BW (Mbps)	$S_{\text{peak}}$ (mJy beam $^{-1}$ )
(a)	10-02-11	EVN	5	1.2	1024	$2.67 \pm 0.26$
(b)	10-02-18	VLBA	6	3.0	512	$0.77 \pm 0.07$
(c)	10-02-23	VLBA	7	6.0	512	$0.60 \pm 0.07$
(d)	10-02-26	VLBA	7	6.0	512	$0.37 \pm 0.06$
(e)	10-03-22	EVN	7	5.0	1024	$0.14 \pm 0.03$
(f)	10-04-25	VLBA	7	6.0	512	$0.43 \pm 0.06$
(g)	10-04-29	VLBA	8	1.6	512	$0.50 \pm 0.10$

**Table 2.** The results of the circular Gaussian model fitting for the VLBI-detected jet components in XTE J1752–223.

Comp.	MJD (d)	Separation (mas)	Position Angle ( $^{\circ}$ )	Flux (mJy)
A	55238.40	$561.6 \pm 0.4$	$-51.3 \pm 0.1$	4.35
A	55245.58	$618.2 \pm 0.5$	$-50.4 \pm 0.1$	2.20
A	55250.60	$647.1 \pm 0.6$	$-51.2 \pm 0.1$	2.32
A	55253.60	$662.2 \pm 0.8$	$-51.0 \pm 0.1$	1.05
B	55253.60	$173.8 \pm 0.8$	$-49.9 \pm 0.3$	0.86
C	55277.23	$259.6 \pm 1.8$	$-53.5 \pm 0.4$	0.75
D	55311.46	$0.0 \pm 0.6$		0.43
D	55315.56	$3.2 \pm 1.2$	$-130 \pm 32$	0.50

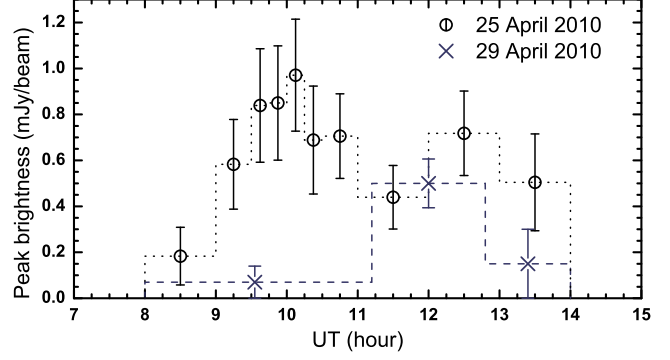
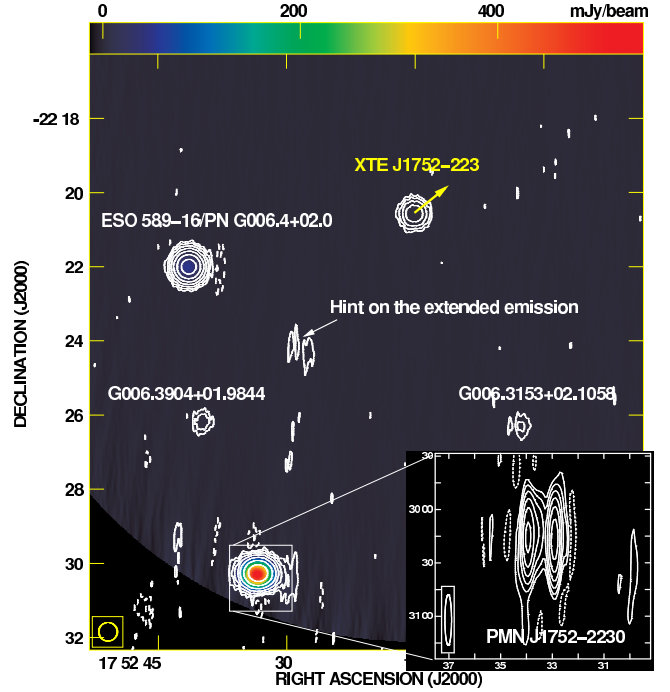
All the experiments used the same phase-referencing source (PMN J1755–2232) and the same duty-cycle. The VLBI calibration procedure was identical as well, and it is described in Paper I. We note that the new EVN observations show a weak extended jet in the calibrator source, but since the radio core accounts for  $\sim 90\%$  of the emission, this extension did not have a significant effect on the phase calibration in the first four epochs. In the WSRT data, we did self-calibration on PMN J1755–2232 and applied the solutions to the target.

### 3 VLBI AND WSRT IMAGING RESULTS

#### 3.1 VLBI detection of multiple jet features

The VLBI total intensity images of XTE J1752–223 are shown in Figure 1. The associated image parameters and Gaussian model-fitting results are listed in Table 1 and 2. There are totally four jet features detected along the position angle of around  $-51^{\circ}$  and marked as A, B, C and D. Components A and B have been reported in Paper I. The EVN image in Figure 1e has achieved a sensitivity of  $1\sigma = 0.03$  mJy beam $^{-1}$ , a factor of two better than other images, and revealed another weak ejecta component C with the peak brightness of  $0.14$  mJy beam $^{-1}$ . Another jet feature, component D, is clearly seen on 2010 April 25 in Figure 1f, but it was initially not detected on 2010 April 29. However, it is present clearly during part of the last observations, at exactly the same position as four days earlier. This indicates that the component has no detectable proper motion, and it is likely variable.

The variation of the image peak brightness during the last two VLBI experiments is shown in Figure 2. To pinpoint the peak time, a variable bin length was used. On 2010 April 25, the image peak brightness of XTE J1752–223 boosted by a factor of five from the non-detection in the first 1-hour bin (8:00 – 9:00 UT) to  $4\sigma$  detection in a 15-minute bin


**Figure 2.** VLBI image peak brightness variation. The dotted and dashed lines are the length of each bin.

**Figure 3.** The WSRT total intensity image of the field of XTE J1752–223. The yellow arrow highlights the jet direction. The contours start from  $3\sigma = 0.24$  mJy beam $^{-1}$  and increase by a factor of 2. The pseudo color image shows the prime beam-corrected intensity distribution.

(10:00 – 10:15 UT). After that, there was no significant decaying. A hint on variability was seen again on 2010 April 29. The source was not detected in the first 2.5 hours. While, it was detected at  $5\sigma$  during 11:10 – 12:48 UT as shown in Figure 1g. The position difference from the previous detections is within the  $3\sigma$  error circle. Note that the variation of the  $uv$ -coverage does not affect the peak brightness in the case of a compact source.

#### 3.2 WSRT imaging of the XTE J1752–223 field

The WSRT image is shown in Figure 3. To show possible extended emission, a circular restoring beam with a size  $30''$  was used. The transient XTE J1752–223 is a point source with a total flux density  $2.8 \pm 0.2$  mJy.

We also detected four other radio sources within the telescope primary beam. The small panel in Figure 3 shows the symmetric double morphology in the extragalactic source PMN J1752–2230 (Saikia et al. 2004) obtained with the original synthesized beam:  $28'' \times 4''$ . The eastern bright source is associated with the planetary nebula ESO 589 – 16 (PN G006.4+02.0) at the distance of 5.1 kpc (Stanghellini et al. 2008). The remaining sources are two stars associated with the *Spitzer* GLIMPLSE (Galactic Legacy Infrared Mid-Plane Survey Extraordinaire, Benjamin et al. 2003) sources G006.3904+01.9844 and G006.3153+02.1058 within its  $3\sigma = 1''$  circle.

#### 4 PROPER MOTION IN TRANSIENT JETS

Component A showed a proper motion decreased from  $9.2 \pm 0.2 \text{ mas d}^{-1}$  to  $4.0 \pm 0.2 \text{ mas d}^{-1}$ , as revealed by Paper I. To check if a significant proper motion can be detected in component B during the only experiment when it was detected, we split the VLBA data obtained on 2010 February 26 into various bins with different lengths. First we made two 3-hour bins and fitted for the position of the component. In addition, we probed bin sizes of 1 hour that provide larger separation between the centre of the first and the last bins. But in this case the four central bins had to be merged due to the low signal to noise ratio of the data (missing short spacings at that time range). Thus the position of component B was obtained for these additional three bins: the first hour, the central four hours, and the last 1 hour of data. We flagged out the high-noise data from Owens Valley (due to a warm receiver) and Brewster in the first half an hour (due to the low elevation); and left the radius, position angle and flux as free parameters to strengthen the conversion of the model fitting.

The angular separation versus time is displayed in the left panel of Figure 4 and listed in Table 3. Component B had a position shift of  $\sim 9 \text{ mas}$  along jet direction within 5 hours. The linear least-square fit, plotted as a straight line, gives a proper motion of  $34 \pm 9 \text{ mas d}^{-1}$  with a reduced  $\chi^2 = 0.4$ . Since the precise position error is unknown, we scaled the errors with the square root of the reduce  $\chi^2$  to estimate the proper motion error. Clearly, component B had a much higher proper motion than component A. The measurements for both components are plotted in the bottom panel of Figure 1 as well.

Alternatively, we searched for the proper motion by measuring the peak brightness of the image after the visibility data were corrected for a range of apparent velocities. Since the high proper motion obtained above smears the component structure during the observations lasting for 6 hours, one should expect to see an increased peak brightness near the real value. The correction along the jet direction was implemented via the AIPS (Greisen 2003) task CLCOR<sup>1</sup>. We used pure natural weighting to make the dirty map, and looked for the peak position within component B. Before applying the proper motion correction to the  $uv$ -data, we removed component A with the AIPS task UVMOD from

**Table 3.** The circular Gaussian model fitting results of component B in different UT ranges.

UT Range (hh:mm)	Separation (mas)	Position Angle ( $^\circ$ )	Flux (mJy)
11:30 – 14:30	$173.1 \pm 2.5$	$-50.1 \pm 0.9$	0.06
14:30 – 17:30	$174.7 \pm 2.5$	$-49.8 \pm 0.9$	0.10
11:30 – 12:30	$169.7 \pm 2.5$	$-50.0 \pm 0.9$	0.10
12:30 – 16:30	$175.8 \pm 2.5$	$-49.1 \pm 0.9$	0.07
16:30 – 17:30	$178.5 \pm 2.5$	$-49.4 \pm 0.9$	0.11

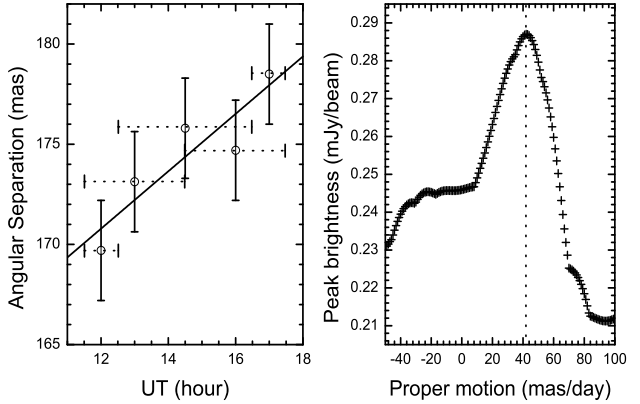


**Figure 4.** Proper motion in the XTE J1752–223 component B. The straight line in the right panel shows the least-square fitting results:  $34 \pm 9 \text{ mas d}^{-1}$ . Note that the horizontal dotted line crossing each data point gives the bin length. The right panel shows the variation of the peak brightness after applying a series of proper motion corrections along the jet direction, as described in the text.

the calibrated visibility data, to avoid any potential interference from its sidelobes.

The variation of the image peak brightness versus the proper motion is plotted in the right panel of Figure 4. The peak brightness has an increase of 17% at a proper motion  $42 \pm 7 \text{ mas d}^{-1}$ , marked with a dotted line. The proper motion error was estimated using its position error and the total observing time. The latter indirect measurement agrees well with the previous direct determination within  $1\sigma$  error.

Components C and B are unlikely to correspond to the same jet feature because the mean proper motion ( $\sim 3.6 \text{ mas d}^{-1}$ ) between the two epochs is much smaller than that observed in component B. We also tried to estimate proper motion in component C using these two methods. Due to the limited sensitivity, we failed to achieve a meaningful result.

## 5 DISCUSSION

### 5.1 The compact jet

Component D was found to have no detectable proper motion with respect to the reference source at the last two VLBI epochs. The only explanation for this is that component D is the radio core of the system. We note that Miller-Jones et al. (2011) arrived to the same conclusion first: they independently analyzed data from the last two VLBA epochs, and showed that component D was positionally consistent

<sup>1</sup> Note that the reference time is at 0:00 UT of the first observing day instead of the mid-point of the VLBI experiment in AIPS, and this had to be taken into account as well.

with the optical counterpart of XTE J1752–223, within a  $1\sigma = 46$  mas error circle. They had only a  $3.5\sigma$  detection on 2010 February 29. In our analysis, we obtained a considerably higher significance of the detection reaching  $5\sigma$ , firmly establishing that component D is related to the core region/compact jet in XTE J1752–223 and not related to a new transient ejecta.

Compared with the most sensitive EVN observations of 2010 March 22 during the X-ray soft state, the radio core re-brightened by a factor of  $>10$ . The non-detection in the earlier soft state is unlikely caused by the fast variability because the core was not detected on short time scales. The re-appearance provides a rare case of direct detection of the re-activation of radio emission in the compact jet during the soft to hard X-ray state transition, as described by the unified model for the coupling of accretion and ejection in black hole X-ray binaries (Fender et al. 2009). In fact, *RXTE* observations on 2010 March 27 have revealed XTE J1752–223 in transition from the soft to the hard state (Muñoz Darias et al. 2010).

The compact jet appears highly variable. However, we note that the declination of the source is low and the strong apparent variation might be due to poor tropospheric conditions especially at the beginning and end of the observations, when the source elevation was very low. However the ATCA observations did show significant variations on timescales of days (Brocksopp et al., in prep.). In literature, strong daily variations were also observed in XTE J1720–318 in the post low hard state (Brocksopp et al. 2005). Significant flux density variation on shorter ( $< 1$  day) time scale were seen in GRS 1915+105 (Fender et al. 1999) and XTE J1650–500 (Corbel et al. 2004).

## 5.2 Relativistic ejections

According to the new proper motion measurements, component B is a transient jet component moving toward the same direction as component A (cf. Paper I), in agreement with the core location discussed above. Although we could not measure the proper motion of component C in the same way as component B, it lies between components A and B which indicates that there were at least three ejection events revealed by the VLBI observations during the 2010 outburst of XTE J1752–223.

The source shows a profound one-sided morphology, unprecedented for X-ray black hole binaries with transient ejecta. We searched for the receding jet in the VLBI images including the deep EVN image. There were no receding ejecta found. If component A was ejected during the major X-ray outburst around MJD 55218, a mean proper motion of  $\sim 28$  mas d $^{-1}$  is required to explain the large angular separation from the assumed core. Considering the low proper motion of  $\leq 10$  mas d $^{-1}$  observed at the later stage, component A must have an extremely high proper motion at the early stage. The high proper motion observed in component B, an ejecta much closer to the core than component A, indirectly supports the association of component A with the major outburst. As a relativistic jet usually evolves with a decaying luminosity after the ejection, the non-detection of component B observed three days earlier is unlikely due to the insufficient sensitivity. Assuming component B was ejected around MJD 55250.6 (during another flare, Brocksopp et

al. in prep.), its average proper motion is  $\sim 58$  mas d $^{-1}$ , in agreement with our measurements.

Component B has a high apparent speed of  $\sim 0.7$  c if it is at 3.5 kpc as estimated by Shaposhnikov et al. (2010) via the spectral-timing correlation scaling technique (model-dependent). However, if the source is located at a larger distance, e.g. near the Galactic centre, then XTE J1752–223 might be another example of superluminal Galactic jets, such as GRS 1915+105 (Mirabel & Rodríguez 1994; Fender et al. 1999) and GRO J1655–40 (Tingay et al. 1995; Hjellming & Rupen 1995). Taking into account that component B might have already somewhat decelerated by the time it was detected, XTE J1752–223 is a promising Galactic superluminal source candidate. The resulting Doppler deboosting effect may be responsible for the non-detection of the receding transient jets, a rarely-seen property in stellar mass black hole binaries.

## 5.3 A hint on the extended emission

There might be an extended emission in rough agreement with the position angle of the transient jet between XTE J1752–223 and G006.3904+01.9844 in Figure 3. Such the extended emission might be a large-scale diffuse relic emission associated with the transient. As the limited sensitivity  $3\sigma = 0.25$  mJy beam $^{-1}$ , deep observations at lower frequencies are required to confirm its existence. A jet-blown bubble,  $\sim 5$  pc in diameter, is found in Cygnus X-1 (Gallo et al. 2005). It is inferred that there exists a cavity surrounding microquasars (Hao & Zhang 2009). As XTE J1752–223 showed strong jet decelerations, it is a promising candidate for the deep observations to hunt for the extended emission region.

## 6 CONCLUSIONS

We investigated the proper motion of the closest ejecta to the assumed core among the detected transient jet components in the 2010 outburst of XTE J1752–223. Besides measuring proper motion through splitting the experiment into a few time bins, we looked for a proper motion via monitoring the variation of the image peak brightness of the proper motion-corrected visibility data. Both ways give a very high proper motion and imply that the ejections are at least mildly relativistic. We also reported the detection of another new ejecta observed at the end of 2010 March. We provided another independent VLBI identification of the compact jet and have shown that it might be highly variable. Moreover, we found a hint on the large-scale extended emission in the field of XTE J1752–223 with the WSRT observations.

## ACKNOWLEDGMENTS

We thank the EVN Programme Committee and the VLBA Proposal Selection Committee for prompt approval of our observations. e-VLBI developments in Europe were supported by the EC DG-INFOS funded Communication Network Developments project EXPReS. The National Radio Astronomy Observatory is a facility of the National Science Foundation operated under cooperative agreement by Associated Universities, Inc. The EVN

is a joint facility of European, Chinese, South African and other radio astronomy institutes funded by their national research councils. The WSRT is operated by ASTRON with support from the Netherlands Foundation for Scientific Research.

## REFERENCES

- Benjamin R.A. et al., 2003, *PASP*, 115, 953  
 Brocksopp C. et al., 2005, *MNRAS*, 356, 135  
 Brocksopp C. et al., 2009, *Astronomer’s Telegram*, 2278  
 Brocksopp C. et al., 2010, *Astronomer’s Telegram*, 2400  
 Corbel S. et al., 2004, *ApJ*, 617, 1272  
 Curran P.A. et al., 2011, *MNRAS*, 410, 541  
 Fender R.P. et al., 1999, *MNRAS*, 304, 865  
 Fender R.P. et al., 2004, *MNRAS*, 355, 1105  
 Fender R.P. et al., 2009, *MNRAS*, 396, 1370  
 Gallo E. et al., 2005, *Nature*, 436, 819  
 Greisen E.W., 2003, in Heck A., ed., *Information Handling in Astronomy: Historical Vistas*, *ASSL*, 285, 109  
 Hao J.F. & Zhang S.N., 2009, *MNRAS*, 702, 1648  
 Hjellming R.M., Rupen M.P., 1995, *Nat*, 375, 464  
 Miller-Jones J.C.A. et al., 2011, *MNRAS*, 415, 306  
 Mirabel I.F., Rodríguez L.F., 1994, *Nat*, 371, 46  
 Muñoz Darias T. et al., 2010, *Astronomer’s Telegram*, 2518  
 Nakahira S. et al., 2010, *PASJ*, 62, L27  
 Saikia D.J. et al., 2004, *MNRAS*, 354, 827  
 Shaposhnikov N. et al., 2010, *ApJ*, 723, 1817  
 Shepherd M.C. et al., 1994, *BAAS*, 26, 987  
 Stanghellini L. et al. 2008, *ApJ*, 689, 194  
 Tingay S.J. et al., 1995, *Nat*, 374, 141  
 Yang J. et al., 2010, *MNRAS*, 409, L64

This paper has been typeset from a  $\text{\TeX}$ / $\text{\LaTeX}$  file prepared by the author.